Proc. Natl. Acad. Sci. USA
Vol. 80, pp. 7515–7519, December 1983
Biophysics

Evidence for cross-bridge order in contraction of glycerinated skeletal muscle

(model independent/linear dichroism/dipole moment)

T. P. BURGHARDT†, T. ANDO†, AND J. BOREJDO†‡

†Cardiovascular Research Institute, University of California, San Francisco, CA 94143; and ‡Polymer Department, The Weizmann Institute of Science, Rehovot, Israel 76100

Communicated by Manuel F. Morales, September 2, 1983

ABSTRACT **The linear dichroism of iodoacetylrhodamine labels attached to the single reactive thiol groups of myosin heads was measured to determine the spatial orientation of myosin cross-bridges in single glycerinated skeletal muscle fibers. We have shown previously that in rigor the chromophoric labels are well ordered and assume an orientation nearly perpendicular to the fiber axis; in the presence of MgADP, a large fraction of probe remains well ordered but the probe attitude assumes a more slanted orientation; in relaxed muscle, the probe order is largely lost, implying a high degree of cross-bridge disorder. In this paper, we report that during isometric contraction a large fraction of the probe shows a high degree of order, suggesting the attachment of ≈65% of the cross-bridges to actin. These ordered cross-bridges have a probe attitude similar to that of the MgADP-induced static state and hence are in a mechanical state quite distinct from rigor.**

In seeking a molecular explanation of how force is generated in muscle at the expense of ATP hydrolysis, a particular hypothesis has seemed to rationalize many of the biochemical and physiological data. In this hypothesis, myosin cross-bridges (S-1 moieties of the myosin molecules) are assumed to deliver mechanical impulses to adjacent actin filaments in a cyclical manner. The unitary impulses are assumed to result from the interaction of nucleotides with enzymatic sites on the cross-bridges (1). One of the potentially powerful methods of studying these events consists of recording spectroscopic data from dipolar (fluorescent or paramagnetic) probes residing in, or artificially attached to, the cross-bridges (2). Recently, investigators using directional EPR to monitor the orientation of spin labels attached to cross-bridges have concluded that, during the generation of isometric tension, only a small fraction (20%) of the cross-bridges are attached to actin while the rest are unattached (3). Moreover, they concluded that the predominant probe orientation is identical to that of rigor, suggesting that those cross-bridges that are attached to actin have the rigor-state orientation. These findings imply that the cross-bridge, or a domain of the cross-bridge where the probe is attached, maintains a constant orientation during force generation. In this work, we have observed the active state by using a method based on the absorption dichroism of fluorescent probes attached to the cross-bridges in single fibers (4). Our data suggest that ≈65% of the cross-bridges are attached to actin and that those that are attached to actin do not have the rigor-state orientation but have an orientation characteristic of a nucleotide-ligated state that can be simulated statically by addition of MgADP.

The publication costs of this article were defrayed in part by page charge payment. This article must therefore be hereby marked "*advertisement*" in accordance with 18 U.S.C. §1734 solely to indicate this fact.

THEORY

The linear dichroism technique for measuring the spatial orientation of cross-bridges in a muscle fiber has been described (4). In this section, we outline the central points of the optical technique wherein the total emitted fluorescence is used to measure the absorption of the fluorescent probe and introduce a model-independent method for interpreting the data.

In previous modeling of dichroism (and also fluorescence polarization) data, it was assumed that the dipolar probes are distributed in some plausible geometry and the effects expected to be observed were predicted and then compared with actual observations. There is nothing incorrect with this procedure but it does not clearly establish what general features of the geometry of the dipole distribution can be determined. In this paper, we will, as usual, be interested in developing equations applicable to data to deduce the attitudes of the dipoles in the muscle fiber but we shall also be interested in answering such questions as the number and type of parameters determined by data of this kind. To investigate the latter questions, we focus on the formal aspects of the problem, such as symmetry in the fiber and the form of the equations describing the interaction of the excitation light with the absorption dipole moment. The approach to be taken is thus less familiar and more cumbersome but, in the end, we will be rewarded with results that cannot be obtained unambiguously by the usual approach.

Linear Dichroism. The unit absorption dipole moment, α, of a chromophore and the incident plane-polarized excitation light propagating along the x axis with electric field polarization given by $E = (0,\sin\psi,\cos\psi)$ are shown in Fig. 1. The unit absorption dipole moment with polar angle θ and azimuthal angle ϕ is $\alpha = (\sin\theta\cos\phi,\sin\theta\sin\phi,\cos\theta)$. The z axis is taken as the fiber axis. The absorption of excitation light by α is proportional to $(\alpha E)^2$, where (4)

$$(\alpha E)^2 = \sin^2\theta\sin^2\phi + (\cos^2\theta - \sin^2\theta\sin^2\phi)\cos^2\psi + 2\sin\theta\cos\theta\sin\phi\sin\psi\cos\psi. \quad [1]$$

In a labeled muscle fiber, we are dealing with many probes, and *a priori* we do not know by what θ and ϕ each of these probes is characterized. To describe the situation, we can invent a distribution function, $N(\theta,\phi)$, that tells the fraction of the total number of probes that is characterized by each θ,ϕ pair in the admissible ranges of θ and ϕ. The number of probes characterized by θ,ϕ is thus $N\sin\theta d\theta d\phi$; if we sum the absorbance contributions of all such elements, we obtain the ob-

Abbreviations: Ap_5A, P^1,P^5-diadenosine-5′-pentaphosphate; IATR, iodoacetamidotetramethylrhodamine; S-1, myosin subfragment 1.

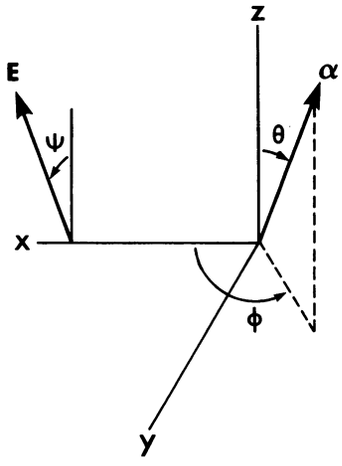

FIG. 1. Geometry of the dichroism experiment. α is the absorption dipole moment of the chromophore with the polar angle θ and the azimuthal angle ϕ. The linearly polarized electric field, E, is propagating along the x axis and forms angle ψ with the z axis. The z axis is parallel to the fiber axis.

servable absorbance of the system:

$$A = \int_{\Omega_0} \sin\theta d\theta d\phi N(\theta,\phi)(\alpha\cdot E)^2, \qquad [2]$$

where Ω_0 is the unit sphere. Instead of assuming in advance that the probes have a particular distribution in the fiber, we acknowledge only that N will depend on θ and ϕ and that it will reflect something of the fiber shape in relation to the arrangement of the experiment. On the basis of these considerations, we assume only that N is a function expandable in a complete set of orthonormal functions. The choice of orthonormal functions is suggested by the symmetry of the system and the experimental technique used. A reasonable choice for describing the linear dichroism of a muscle fiber is the set of spherical harmonics $Y_{l,m}(\theta,\phi)$, because the dipolar system is most easily described in spherical coordinates on the unit sphere and because the absorption A (Eq. 2) is composed of only a few of the distribution moments in the expansion of $N(\theta,\phi)$ in terms of $Y_{l,m}(\theta,\phi)$. The latter feature is a consequence of Eq. 2 and the form of the interaction of the electric dipole moment with an electromagnetic field (see below).

The expansion of the distribution function $N(\theta,\phi)$ is

$$N(\theta,\phi) = \sum_{l=0}^{\infty}\sum_{m=-l}^{l} d_{l,m}Y_{l,m}(\theta,\phi), \qquad [3]$$

where the $d_{l,m}$ are distribution moments independent of θ and ϕ. The single dipole absorption $(\alpha\cdot E)^2$ must also be a sum of $Y_{l,m}$ but finite and can be shown from Eq. 1 to have the explicit form

$$(E\cdot\alpha)^2 = \omega + \mu\cos^2\psi + \nu\sin\psi\cos\psi, \qquad [4]$$

where $\omega = (4\pi/9)^{1/2}Y^*_{0,0} - (4\pi/45)^{1/2}Y^*_{2,0} - (2\pi/15)^{1/2}(Y^*_{2,2} + Y^*_{2,-2})$, $\mu = (4\pi/5)^{1/2}Y^*_{2,0} + (2\pi/15)^{1/2}(Y^*_{2,2} + Y^*_{2,-2})$, and $\nu = -2i(2\pi/15)^{1/2}(Y^*_{2,1} + Y^*_{2,-1})$. Substituting Eqs. 3 and 4 into Eq. 2 and using the orthogonality condition $(\int_{\Omega_0}\sin\theta d\theta\, d\phi Y^*_{l,m}Y_{l',m'} = \delta_{l,l'}\delta_{m,m'}$, where $\delta_{i,j}$ is the Kronecker *delta* and * means complex conjugate), we find that the linear dichroism signal is

$$A = \gamma + \beta\cos^2\psi + \varepsilon\sin\psi\cos\psi, \qquad [5]$$

where $\gamma = (4\pi/9)^{1/2}d_{0,0} - (4\pi/45)^{1/2}d_{2,0} - (2\pi/15)^{1/2}(d_{2,2} + d_{2,-2})$, $\beta = (4\pi/5)^{1/2}d_{2,0} + (2\pi/15)^{1/2}(d_{2,2} + d_{2,-2})$, and $\varepsilon = -2i(2\pi/15)^{1/2}(d_{2,1} + d_{2,-1})$. The coefficients γ, β, and ε relate linearly independent functions of ψ to the dichroism signal. Measurement of A as a function of ψ will determine γ, β, and ε; these coefficients in turn are related to the model-independent distribution moments $d_{i,j}$.

It can be seen from Eq. 5 that only moments with $l = 0$ and $l = 2$ contribute to the linear dichroism signal. Moments of order $l = 1,3,4, \ldots$ are not "seen" with this technique. Thus distribution functions containing both contributing and "unseen" moments, such as gaussian or delta function distributions, cannot be uniquely specified by linear dichroism experiments.

Data Analysis. The signal A is proportional to the quantum efficiency of the fluorescent probe and other factors that are difficult to measure. We circumvent such measurements by normalizing the signal. The normalized absorption, $\bar{A}(\psi) = A(\psi)/A(\psi_0)$ satisfies

$$\bar{A} - 1 = b(\cos^2\psi - \cos^2\psi_0) + c(\sin\psi\cos\psi - \sin\psi_0\cos\psi_0), \qquad [6]$$

where ψ_0 is the excitation polarization angle at which $A(\psi)$ is a maximum, $b = \beta/A(\psi_0)$, and $c = \varepsilon/A(\psi_0)$. With this normalization, however, we lose the information in one of the observables (arbitrarily chosen here to be γ). The observables b and c are linear parameters in the expression for A and are uniquely determined provided there are two measurements of A made at two different values of ψ (yielding two equations for two unknowns).

Typically, $\bar{A}$ is measured at many different ψ values. We then have to find the b and c values for the curve that "best fits" $\bar{A}(\psi) - 1$. Usually this is done with a search-and-compare routine, but we have used a more direct method based on constructing orthogonal functions. If by $\langle m(\psi)n(\psi)\rangle$ we mean $\int_0^\pi m\, n\, d\psi$, we wish to find a pair of functions, $q(\psi)$ and $p(\psi)$, that are orthogonal to the two functions of which $\bar{A}(\psi) - 1$ is a linear combination—i.e., to $f(\psi) = \sin\psi\cos\psi - \sin\psi_0\cos\psi_0$ and $g(\psi) = \cos^2\psi - \cos^2\psi_0$, respectively. We find

$$q(\psi) = (\langle g^2\rangle - \langle fg\rangle^2/\langle f^2\rangle)^{-1}[g(\psi) - f(\psi)\langle fg\rangle/\langle f^2\rangle] \qquad [7]$$

and

$$p(\psi) = (\langle f^2\rangle - \langle fg\rangle^2/\langle g^2\rangle)^{-1}[f(\psi) - g(\psi)\langle fg\rangle/\langle g^2\rangle].$$

From the orthogonality of q and p to f and g, $b = \langle(\bar{A} - 1)q\rangle$ and $c = \langle(\bar{A} - 1)p\rangle$. These "inner products" defining b and c are easily calculated numerically, giving equal weight to all the data points.

MATERIALS AND METHODS

Chemicals. ATP, ADP, P^1,P^5-diadenosine-5′-pentaphosphate (Ap_5A), myokinase, and hexokinase were from Sigma. Iodoacetamidotetramethylrhodamine (IATR) was from Research Organics (Cleveland, OH). All other chemicals were of analytical grade.

Solutions. Rigor solution was 80 mM KOAc/5 mM $MgCl_2$/2 mM EGTA/5 mM Na phosphate buffer, pH 7.0. Sometimes, hexokinase (12 μg/ml), 10 mM glucose, and myokinase (35 μg/ml) were added to it to ensure complete removal of ATP and ADP from the fiber.

Relaxing solution had the same composition as rigor solution except that ATP was added at 4 mM.

In activating solution, 0.1 mM $CaCl_2$ replaced the EGTA of the relaxing solution, and 4 mM phosphocreatine and creatine kinase (0.4 mg/ml) were added to regenerate hydrolyzed ATP. Substrate diffusion problems were not significant in our experiments because the focused laser beam sampled only a small

population of cross-bridges on the surface of single muscle fibers. This was verified by the observation that there were no significant changes in the results when the ATP concentration in the activating solution was varied.

In ADP-containing solution, 4 mM ADP was added to rigor solution, together with 10 mM glucose and hexokinase (100 μg/ml) to remove contaminating ATP, and 100 μM Ap_5A to keep the myofibrillar myokinase from converting ADP to ATP.

Fiber Handling and Characterization. A single fiber, or a bundle of two or three fibers, was prepared from rabbit psoas muscle. The muscles were glycerinated for periods ranging from a day to several weeks in a relaxing water/glycerol solution as described in ref. 5.

The fibers were fluorescence labeled with IATR as described in ref. 4 except that the labeling time was decreased from 1 hr to 15–30 min. The free dye was removed by washing the fibers with relaxing solution for 2–12 hr. With these labeling conditions, the absorption coefficient of a single labeled fiber was estimated to be $\approx$0.02. We observed no systematic difference in results for the fibers when the glycerination period, the labeling time, and the washing time were varied over the time periods given.

After washing, and immediately before an experiment, individual fibers were mounted on a glass slide and immersed in rigor or relaxing solution. At this time, both ends of the fiber were rigidly fixed to the glass with glue. A coverslip was placed over the fiber with two bands of silicone grease placed along the long dimension of the glass slide supporting the weight of the coverslip.

Fibers prepared in this way generated a force per unit area of $\approx$2 kg/cm^2 during contraction. The fibers had sarcomere lengths of 2–2.5 μm. Data for a dichroic curve were collected in less than 5 sec. All active fiber measurements were made within 1 min of the onset of contraction. All experiments were carried out at room temperature.

Dichroism Apparatus. The dichroic instrument was identical to that described in ref. 4 except that an objective with a numerical aperture of 1.4 (Zeiss, Planapo 63X) was used and the orientation of the linear polarization of the excitation light was varied by using a polarization rotator (Spectra Physics, Santa Clara, CA). The image plane diaphragm defined a circular spot of 5 μm on an object plane.

The depolarizing effect of the focusing lens on the polarized laser beam was taken into account by using certain formulas (6, 7) adapted to our experimental conditions (i.e., a ratio of the focusing lens aperture to the incident beam radius of $\approx$1 and an angular aperture of the lens of 90°). We calculated that $\approx$13% of the total light intensity that excites observed fluorescence is polarized in directions other than that of the incoming laser beam. This rather small effect is considered in calculating the tabulated model-dependent results below (model-independent results are not affected).

RESULTS

Dichroic curves were measured for passive and active fibers. Curves for a fiber in rigor, relaxation, in the presence of MgADP, and in the active state are shown in Fig. 2. The average values for the model-independent observables b and c for each of these states are summarized in Table 1. The concavity indicated by the sign of b of all the curves falls into two categories, the "rigor-like" or the "MgADP-like" shape.

The physical interpretation of the coefficients b and c is straightforward. Our data show that $c \approx 0$ for all states. This result shows that the fiber has symmetry under 180° rotation about its axis (in previous work, this feature was considered an assumption). In transitions in which b retains its sign (e.g., rigor $\rightarrow$ relaxed), increases in the magnitude of b indicate increased order. In transitions in which b changes sign (e.g., rigor $\rightarrow$ active), the predominant value of the polar angle θ shifts

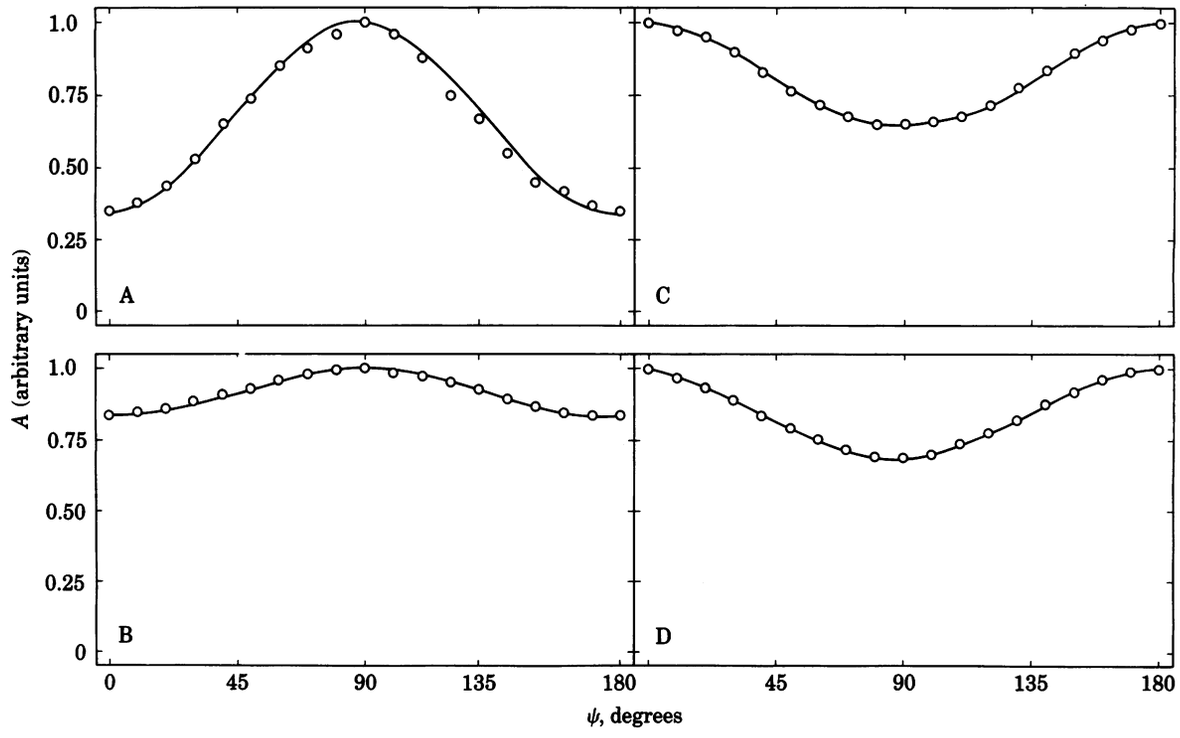

FIG. 2. Typical absorption curves from muscle fiber in rigor (*A*), relaxation (*B*), the MgADP-induced state (*C*), and contraction (*D*). Note that in contraction the concavity of the absorbance is the same as in the MgADP-induced state. Open circles are actual data points and the smooth curve is the theoretical fit. ψ is the angle between the fiber axis and the direction of polarization of the exciting light.

Table 1. Experimental results for the model-independent order parameters b and c and calculated values for the model-dependent parameters θ and h

	Rigor	Relax	MgADP	Active
b	−0.48 ± 0.13	−0.17 ± 0.04	0.23 ± 0.07	0.25 ± 0.06
c	0.0009 ± 0.04	−0.02 ± 0.02	0.006 ± 0.03	0.006 ± 0.04
θ	69°	69°	47°	47°
h	0.68 ± 0.2	0.21 ± 0.05	0.60 ± 0.2	0.65 ± 0.2

Experimental results represent mean ± SD. Values for θ, the polar angle of the ordered chromophores, were calculated for the rigor and ADP-induced state from observations on a fiber irrigated with rhodamine-labeled S-1. The values of θ used in the calculation of h for the relaxed and active states were assumed to be those of the rigor and MgADP-induced states, respectively. The present results for the active state are derived from 52 independent observations on 12 muscle fibers. Previous conclusions indicating no probe order in the active state (4), drawn from four observations, are not confirmed here, for reasons that we do not understand. There is a small difference in values for h and θ above and the values reported earlier (4) because of a computational error in equations 10 and 11 of ref. 4. However, none of the qualitative observations made earlier (such as the "rigor" and "anti-rigor" categorical designations) are altered by the present work.

across the "magic" value, $\theta = 54.7°$.

We can think further about the problem by making certain assumptions about the static states. Suppose that a fraction, h, of the cross-bridges has perfect order, with cylindrical symmetry about the z axis and a unique polar angle θ and that another fraction $(1 - h)$ has a completely random orientation. We may also account for independent motion of the rhodamine group in a cone of half-angle $\eta = 20°$ (4). Then, it can be shown that

$$b = \frac{h\left[3\cos^2\theta\left(2\cos^2\eta - \frac{1}{2}\right) - \frac{1}{2}\cos^2\eta\right]}{\frac{1}{3} + \frac{1}{3}h\,(3\cos^2\psi_0 - 1)\left[\cos^2\theta\left(2\cos^2\eta - \frac{1}{2}\right) - \frac{1}{2}\cos^2\eta\right]}. \quad [8]$$

This model thus assigns two parameters, h and θ, to the single observable b.

It is generally believed that in all physiological states there are comparatively large "bare" zones of thin filaments and that, when fibers are irrigated with S-1, the fragments attach to these bare zones. It is thus plausible that such "exogenous" S-1 assumes whatever binding distribution is appropriate in the imposed ionic environment, unperturbed by disordering influences existing elsewhere. If, for the rigor and ADP-induced states, the rhodamine-labeled S-1 infused into fibers attains complete order ($h = 1$), we can calculate the polar angle θ for these states. These values of θ are then used to calculate the ordered fraction h for fibers in which endogenous S-1 has been labeled with IATR. The rigor value of θ is also used to calculate h for the relaxed state. These results are given in Table 1.

For fibers in rigor and in the presence of MgADP, we believe that the observed randomness (i.e., the fact that on average, $h < 1$) arises from nonspecific labeling of the fiber and from fiber-order damage during preparation.

In relaxation, in agreement with our earlier observations (4, 8) and also with those of Thomas and Cooke (9), we find that the probes are mostly disordered. Nevertheless, some rigor-like component can be seen in relaxed fibers in 80 mM KOAc (Fig. 2*B*). This rigor component can be suppressed by increasing the ionic strength of the relaxing solution.

The dichroism signal in the active state is indistinguishable from that in the static MgADP-induced state (Table 1). If these data are interpreted using the polar angle appropriate to the ADP-induced state polar angle and Eq. 8, then the ordered fraction has the same value as in the MgADP-induced state. This assumption was made to calculate the values of θ and h given in Table 1 for the active state.

DISCUSSION

The present results show that during isometric activity, (*i*) ≈65% of the myosin heads are attached (see below) and (*ii*) the attached heads are ordered and characterized by a probe attitude similar to that induced by ADP in static experiments. These conclusions agree with what has been concluded from x-ray observations of contracting muscle—i.e., a high percentage of actin attachment and a diffraction pattern qualitatively different from that in rigor (10). Our conclusions, however, differ from deductions from EPR work that suggest ≈20% cross-bridge attachment and spectra indistinguishable from rigor spectra (3). The origin of these differences is not clear at present: even among probes covalently linked to the same (SH-1) thiol, sensitivity to a given process can vary widely. For example, the probe attitude induced by ADP is sensitively detected by IATR, poorly detected by iodoacetylfluorescein, and not detected by either 5-iodoacetamidoethylaminonaphthalene-1-sulfonic acid or spin labels; it is therefore not surprising that in the active state spin labels do not report an ADP-like state. The molecular origin of these differences among spectroscopic probes is unclear; it could be differences in the protein region on which the sensor moiety of the probe resides (4) or vectorial differences in the relation between the probe dipole and components of the motion. Yet another difference could reside in the extent to which modification of the rapidly reacting thiol (SH-1) of myosin affects the rate of ADP dissociation from the acto–myosin complex. We have compared the rate of ADP dissociation from the acto–myosin complex in solution for modified (with rhodamine) vs. unmodified S-1. We have found no change in the dissociation rate.

Two lines of argument suggest that the oriented component observed during isometric contraction arises from the fraction of cross-bridges that are attached to actin: first, the attached cross-bridges in other states (i.e., rigor) are highly ordered while the detached ones, as in relaxation, are largely disordered. Similarly, fibers stretched beyond overlap give dichroism that is indistinguishable in rigor and in relaxing solution, suggesting a tight correlation between binding to actin and the degree of probe organization. Second, the detached cross-bridges are highly mobile (11) and any residual order present that appears as well-developed myosin-based layer lines in x-ray diffraction experiments (12) will give a rigor-like dichroism. It is therefore likely that any order in the probe distribution other than rigor has to be imposed on the cross-bridges by actin.

The oriented state that we observe in contraction can be predominant if the transition from this state to the subsequent state is rate limiting in the overall cross-bridge cycle. Cross-bridge dissociation and reattachment to actin are too rapid to be rate limiting during isometric tension development (13). It therefore appears that the transition from our predominant oriented state to the subsequent state, possibly the force generating state, is rate limiting. It is also relevant that analysis of the fluctuations in polarized fluorescence revealed the presence of very slow rotational motions during isometric contraction of the rhodamine-labeled fibers (5); in view of the present results, the fluctuation analysis may have isolated the rotational motion associated with the rate-limiting transition following the predominant state observed here. If so, then this transition occurs at a frequency of 1–2 Hz.

While our results show unequivocally that the predominant probe attitude during isometric activity is not that of rigor but is indistinguishable from that statically imposed by MgADP, they cannot yet be clearly related to underlying chemical events or to force generation. The obstacle is a seeming conflict between various fiber and solution experiments: specifically, although in solution MgADP binding to S-1 markedly affects actin ligation, addition of MgADP to a fiber in rigor alters the IATR attitude but, at "physiological" ionic strength, it seems not to affect the tension (4) or the small angle x-ray diffraction pattern (14). On the basis of the fiber observations, it is difficult to see how the ADP state–rigor transformation could be the actual power stroke. Possible explanations are that (*i*) the rigor state is not really the end of the power stroke but an artificially induced state without physiological importance or (*ii*) there exists another intermediate short-lived attached state following our ADP state (which cannot be induced by simply adding ADP) and the transition from this state to rigor is the true power stroke.

We thank Prof. M. F. Morales for helpful suggestions and Ms. Carroll Flynn for technical assistance. The research was supported by Grants HL-16683 from the U.S. Public Health Service, PCM-7922174 from the National Science Foundation, and CI-8 from the American Heart Association, and by a grant from the U.S.–Israel Binational Science Foundation. T.P.B. is a Career Investigator Fellow of the American Heart Association, T.A. was for a time a Fellow of the Muscular Dystrophy Association, and J.B. is an Established Investigator of the American Heart Association.

1. Morales, M. F., Borejdo, J., Botts, J., Cooke, R., Mendelson, R. A. & Takashi, R. (1982) *Annu. Rev. Phys. Chem.* **33**, 319–351.
2. Aronson, J. F. & Morales, M. F. (1969) *Biochemistry* **8**, 4517–4522.
3. Cooke, R., Crowder, M. S. & Thomas, D. D. (1982) *Nature (London)* **300**, 776–778.
4. Borejdo, J., Assulin, O., Ando, T. & Putnam, S. (1982) *J. Mol. Biol.* **158**, 391–414.
5. Borejdo, J., Putnam, S. & Morales, M. F. (1979) *Proc. Natl. Acad. Sci. USA* **76**, 6346–6350.
6. Burghardt, T. P. & Thompson, N. L. (1984) *Opt. Eng.*, in press.
7. Yoshida, A. & Asakura, T. (1974) *Optik* **41**, 281–293.
8. Borejdo, J. & Putnam, S. (1977) *Biochim. Biophys. Acta* **459**, 578–595.
9. Thomas, D. D. & Cooke, R. (1980) *Biophys. J.* **32**, 891–906.
10. Huxley, H. E., Simmons, R. M., Faruqi, A. R., Kress, M., Bordas, J. & Koch, M. H. J. (1981) *Proc. Natl. Acad. Sci. USA* **78**, 2297–2301.
11. Thomas, D. D., Ishiwata, S., Seidel, J. C. & Gergely, J. (1980) *Biophys. J.* **32**, 873–890.
12. Huxley, H. E. & Brown, W. (1967) *J. Mol. Biol.* **30**, 383–434.
13. Goldman, Y. F., Hibberd, M. G., McCray, J. A. & Trentham, D. R. (1982) *Nature (London)* **300**, 701–705.
14. Rodger, C. D. & Tregear, R. T. (1974) *J. Mol. Biol.* **86**, 495–497.